Spallation in the Alloy Ti-6Al-4V

Cite as: AIP Conference Proceedings **620**, 511 (2002); https://doi.org/10.1063/1.1483589
Published Online: 03 July 2002

P. D. Church, T. Andrews, N. K. Bourne, and J. C. F. Millett

CP620, *Shock Compression of Condensed Matter – 2001*
edited by M. D. Furnish, N. N. Thadhani, and Y. Horie

SPALLATION IN THE ALLOY Ti-6Al-4V

P.D. Church, T. Andrews N.K. Bourne*, J.C.F. Millett*,

DERA, Fort Halstead, Sevenoaks, Kent, TN14 7BP, UK.
**Royal Military College of Science, Cranfield University, Shrivenham, Swindon, SN6 8LA, UK.*

Abstract The dynamic tensile (spall) strength of the common engineering titanium alloy Ti-6Al-4V has been investigated as a function of impact stress and specimen thickness under conditions of symmetrical impact. Flyer and target plate geometries have been controlled such that release fans from the rear of the flyer and the target meet in the middle of the target plate. Whilst it has been generally assumed that specimen geometry has no effect upon the resultant spall strength, all other conditions being equal, computer modelling has suggested otherwise. It is the purpose of this paper to investigate these effects experimentally and theoretically.

INTRODUCTION

The interaction of release waves from flyer and target plates during plate impact experiments, resulting in tensile failure or spall has been a subject of interest for many years. Recently, attention has focussed upon engineering materials such a titanium alloys. Razorenov et al [1] observed that the spall strength of the common engineering alloy Ti-6Al-4V did not change with varying oxygen content. Dandekar and Spletzer [2] showed that the Hugoniot Elastic Limit was dependant upon specimen thickness (precursor decay). Additionally, they also demonstrated that the spall strength also depended on thickness, contrary to first order spall theory. In a wider context, spall strength has also been shown to be sensitive to aniosotropy, either due to preferred orientation of the grain structure [3], or due to directional distribution of second phases [4]. Therefore, it can be seen that whilst spall has been investigated thoroughly, present theories are as yet unable to accurately predict the spall behaviour of common engineering materials. The aim of this work is to present spall experiments in Ti-6Al-4V, and compare results with simulations.

EXPERIMENTAL

Plate impact experiments were carried out in two configurations but in both cases the impacts were symmetric. In the first a 3 mm flyer plate impacted a 6 mm thick target, whilst in the second a 6 mm flyer impacted a 12 mm target. These were samples were impacted at above their HELs at two stress levels to observed spall signals at different stress levels and uniaxial strain compression and release waves were recorded after travel through tiles. Prior to impact an adjustable specimen mount was used to carefully align the sample parallel to the flyer to better than 1 mrad.

Specimens were backed with 12 mm thick polymethylmethacrylate (PMMA) blocks and the longitudinal stress normal to the plane wave fronts was measured by a manganin gauge (Micro-Measurements LM-SS-125CH-048) situated at the metal/PMMA interface. PMMA was chosen because it is closely matched in impedance to the epoxy layer and the gauge backing material. It was found that the material punches through the gauge insulation so that a thickened layer was adopted. This indicates the violent nature of conditions at this face compared with more ductile materials. Data were collected on a fast (1 GS s^{-1}) digital storage oscilloscope. The calibration data of Rosenberg *et al.* ([5] were used to reduce the voltage data to stress.

Traces were gathered for each tile thickness with the Hugoniot stress being kept constant for a given purity of ceramic by using the same velocity and impactor material. Velocity was measured to an accuracy of 0.5 % by the use of four sequential sets of shorting pins. Since the gauge measures the transmitted stress wave amplitude in PMMA a correction must be made for the transmission coefficient (T) from alumina to PMMA. This can be expressed in terms of the acoustic impedances (Z_1, Z_2) of the two materials as

$$T = \frac{2Z_1}{Z_1 + Z_2} \quad .$$

In the subsequent figures *the stress recorded within the PMMA backing is presented* and any

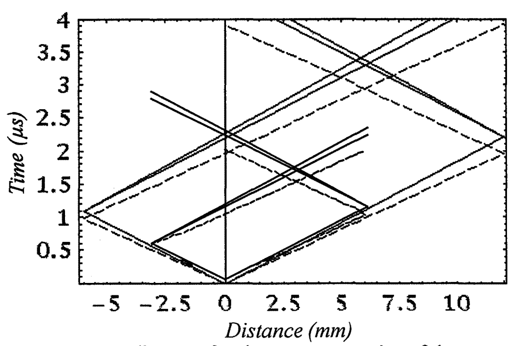

FIGURE 1. *X-t* diagram for the two geometries of the paper.

correction to in-material values is done separately within the text.

Fig. 1 shows a representation of the two impacts at 600 m s^{-1}. The two experiments are self similar and the loading pulse is of twice the duration for the 6 mm flyer than for the 3 mm one. Clearly there is greater separation between elastic and plastic wave fronts for the two cases.

RESULTS

Fig. 2 shows the impacts of 3 mm and 6 mm flyer plates upon 6 mm and 12 mm targets at velocities of 598 and 591 m s^{-1} respectively. There are a further two higher stress traces under identical geometry where the flyer travels at 765 and 781 m s^{-1} These pairs of experiments are presented as representative of a larger series (not all shown) which give similar response to that shown. In particular the spall strength observed is the same as that seen in these experiments.

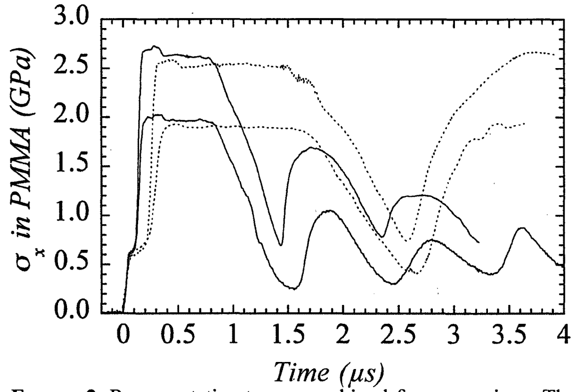

FIGURE 2. Representative traces combined for comparison. The solid traces represent 3 mm hitting 6mm targets and the dotted represent 6 mm hitting 12 mm ones at *ca.* 700 and 800 m s^{-1}.

The lower velocity traces rise to an HEL of 0.7 GPa in all cases. This corresponds to an in-material value of 2.7 GPa for the alloy. Regardless of the distance of travel of the waves or the amplitude of the pulse, this stress remains constant as expected. The signal then rises to its peak and on this point there is a signal riding on top of the pulse of duration *ca.* 150 ns. This feature has no simple explanation at present and further work is underway to explain its origin. The stress then relieves elastically and then plastically and, as is found in the majority of cases, the elastic release is less than the HEL of the material. The release is, in all cases, followed by a reload signal which is different in each case. That for the 3 mm flyer plate corresponds to an in-material value for the stress of 3 GPa which is the spall strength in this configuration. That for the 6 mm impact corresponds to an in-material stress of 5.7 GPa

The two traces at higher velocity show similar features. The HEL is again constant. The stresses achieved are clearly higher but the spall strengths are calculated to be 3.8 and 6.8 GPa respectively. They are in both cases higher than those recorded at the lower velocity.

The increased height of the spall signals at higher velocities may immediately be seen. It will be noted for the 3 mm flyers on 6 mm targets that the rise time of the reload signal is faster than the falling rate of the release. The asymmetry is indicative of the further mechanisms present in the spallation process not yet completely described.

HYDROCODE MODELLING

The main purpose of the modelling studies was to obtain insight into some of the experimental observations and attempt to explain their physical significance. It was clear that some of these observations challenged quite long-standing views of the physics of spallation. Modelling therefore provided a potentially powerful and independent approach to investigating the issues. The main reason for this is that the hydrocodes do not make any pre-determined assumptions concerning the stress-system or wave propagation behaviour. They solve the conservation equations and use constitutive models and equations of state to determine dynamic the material response.

The simulations of these tests were performed using the public domain version of the Lagrangian hydrocode DYNA2D originating from LLNL. The Ti-6Al-4V plate was characterised using the modified Armstrong-Zerilli constitutive model using previously determined coefficients [6]. The fracture model used was based on the Goldthorpe Path Dependent Ductile Fracture Model which attempted to physically link the damage evolution with the constitutive model [7]. The model form is given below:-

$$dS=0.67\exp[1.5\sigma_n-0.04\sigma_n^{-1.5}]d\varepsilon$$

Where σ_n = Stress triaxiality (Pressure/Flow Stress or P/Y)
$d\varepsilon$ = Effective plastic strain
S = Damage

The critical value of failure was 0.5, but there is some uncertainty in this measurement due to the difficulty of analysing the neck formation, which is very severe at low strains.

It is important to realise that the critical failure condition is obtained from a quasi-static tensile test where the pressure/yield (*P/Y*) condition is 0.33. In plate impact spallation tests the strain rate is about 10^6 s^{-1} and the *P/Y* value under uniaxial strain is of the order of 400-800 depending on the impact stress. The model has already been shown to reproduce plate impact VISAR spallation results on iron [8]. Furthermore, the model has given good results for the fracture cylinder test where the strain rate is similar to plate impact, but the stress system is complex 3D and dynamically changing.

MODELLING RE SULTS

All the simulations used a mesh resolution of 0.014mm. These mesh resolutions were sufficient to ensure convergence of the solution and allowed the resolution of all the relevant elastic and plastic waves in the target and flyer. This is necessary to resolve the release fans which cause the spallation. Once the failure condition is reached the element is simply deleted.

The hydrocode predictions for the 3 mm flyers impacting the 6 mm targets are shown in fig 3, over-laid with the experimental results. The predictions are in good agreement for the HEL and the Hugoniot stress level as well as the general pulse length. The release tends to be steeper than the experimental trace indicating an issue with the equation of state. An alternative explanation is that the material responds differently for deformation in tension than compression as in the Bauschinger effect, whereas the hydrocode assumes identical response. The critical failure value used in the

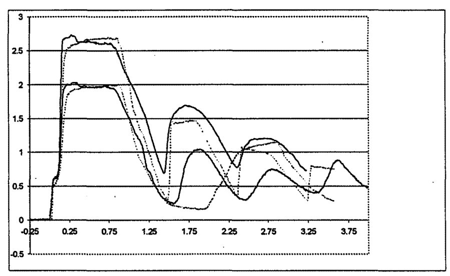

FIGURE 3. Simulation comparison with experiment for 6mm Ti alloy targets. Simulations are dotted line.

Goldthorpe model predicts a full spall failure, though a slightly lower value or change in the bulk sound speed predicts no failure. Therefore the model is suggesting that the material is on the failure threshold . This is supported by the micrographs of these tests, which show isolated void growth or incipient spall. The significance of the model predicting fracture or no fracture is that the material fully unloads before reload which takes a significantly longer time than for the fracture case. It is interesting to note that the best comparison with the experiment is the full fracture case. The model cannot be expected to predict the incipient spall trace as there is no link between damage evolution and the constitutive model. This will be discussed later.

The results for the 6 mm flyers impacting the 12 mm targets are shown in fig 4, compared with the simulations. These tests are more straightforward since the material exhibits a full spall fracture. These simulations raise certain questions, when compared with the experimental results.

The HEL for both the simulated velocities are consistently below the experimental traces. This indicates a degree of precursor decay, primarily due to the strain rate dependency in the model. Reasonable agreement is obtained with the Hugoniot stress and the pulse width. An interesting and unexpected feature is that the release for the lower velocity agrees very well with the experiment. The reload spall signal happens later and the reload pulse bears little resemblance to the experiment. For the upper velocity again the slope of the release is predicted reasonably until the reload signal, which is again much later than the experimental value.

DISCUSSION

This study has demonstrated that the general area of brittle and ductile spallation is not well understood, in detail. Indeed according to classical spall theory the results, by scaling the target and flyer plates should be identical. Clearly the experimental data for this material greatly questions the classical theory. This is not too surprising as merely scaling the geometry, does affect many other aspects in spall, which do not scale.

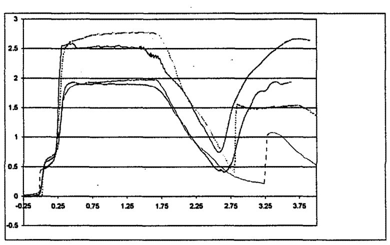

FIGURE 4. Simulation comparison with experiment for 12 mm Ti alloy targets. Simulations are dotted lines.

The release path lengths will be different in the two cases and this leads to significant changes in the momentum and impulse contained within them. By definition this must alter the way in which the voids grow and interact. In addition titanium alloys exhibit large changes of behaviour in tension and compression, even under quasi-static loading and also has a large Bauschinger effect under shock loading. To complicate matters further there is some evidence of brittle as well as ductile fracture.

Other factors in the experiment also shed doubt on well-established views on spallation and wave propagation in general. One of these is the general release behaviour where the slope is significantly different in the thin and thick target plates

Given these factors it is not surprising that hydrocode modelling, using a pure ductile fracture model does not capture all aspects of the experimental data. Clearly more detailed studies are required to gain an understanding of the spallation process in these complicated alloys.

CONCLUSIONS

1. The experiments have demonstrated that spallation does not simply scale with geometry in titanium alloy.
2. The current hydrocode capability cannot reproduce the experimental spall reload signal.
3. Spallation in titanium alloy needs a lot more research to understand the spallation process.

REFERENCES

1. Razorenov, S.V., Kanel, G.I., Utkin, A.V., Bogach, A.A., Burkins, M. and Gooch, W.A., , in *Shock Compression of Condensed Matter 1999,*
2. Dandekar, D.P. and Spletzer, S.V., in *Shock Compression of Condensed Matter 1999,*
3. Edwards, M.R., Bourne, N.K. and Millett, J.C.F.. (2001) These proceedings.
4. Gray, G.T., Lopez, M.F., Bourne, N.K., Millett, J.C.F. and Vecchio, K.S. *These proceedings*. (2001)
5. Rosenberg, Z., Yaziv, D. and Partom, Y. *J. Appl. Phys.* 51 (1980) 3702-3705.
6. Church P, Cornish R, Cullis I, Lynch N, TMS 1998.
7. Goldthorpe B, Jnl de Phys 7, C3 –705, 1997.
8. Church P, Proud B, Andrews T, Goldthorpe B (2001, these proceedings).